Inorg. Chem. **2008**, *47*, 10542−10553

Four-Coordinate Mo(II) as $(silox)_2Mo(PMe_3)_2$ and Its W(IV) Congener $(silox)_2HW(\eta^2\text{-}CH_2PMe_2)(PMe_3)$ (silox = ^{t}Bu$_3$SiO)

David S. Kuiper,[†] Peter T. Wolczanski,*[,†] Emil B. Lobkovsky,[†] and Thomas R. Cundari*[,‡]

Department of Chemistry & Chemical Biology, Baker Laboratory, Cornell University, Ithaca, New York 14853, and Department of Chemistry, Center for Advanced Scientific Computing and Modeling (CASCaM), Box 305070, University of North Texas, Denton, Texas 76203

Received June 27, 2008

The reduction of $[(^t Bu_3SiO)_2MoCl]_2$ (**2**$_2$) provided the cyclometalated derivative, $(silox)_2HMoMo(\kappa\text{-}O,C\text{-}OSi^tBu_2CMe_2CH_2)(silox)$ (**3**), and alkylation of **2**$_2$ with MeMgBr afforded $[(^t Bu_3SiO)_2MoCH_3]_2$ (**4**$_2$). The hydrogenation of **4**$_2$ was ineffective, but the reduction of **2**$_2$ under H_2 generated $[(^t Bu_3SiO)_2MoH]_2$ (**5**$_2$), and the addition of 2-butyne to **3** gave $[(silox)_2Mo]_2(\mu{:}\eta^2\eta^2\text{-}C_2Me_2)$ (**6**), thereby implicating the existence of $[(silox)_2Mo]_2$ (**1**$_2$). The addition of (silox)H to $Mo(NMe_2)_4$ led to $(silox)_2Mo(NMe_2)_2$ (**7**), but further elaboration of the core proved ineffective. The silanolysis of $MoCl_5$ afforded $(silox)_2MoCl_4$ (**8**) and $(silox)_3MoCl_3$ (**9**) as a mixture from which pure **8** could be isolated, and the addition of THF or PMe_3 resulted in derivatives of **9** as $(silox)_2Cl_3MoL$ (L = THF, **10**; PMe_3, **11**). Reductions of **11** and $(silox)_2WCl_4$ (**15**) in the presence of excess PMe_3 provided $(silox)_2Cl_2MPMe_3$ (M = Mo, **12**; W, **16**) or $(silox)_2HW(\eta^2\text{-}CH_2PMe_2)PMe_3$ (**14**). While "$(silox)_2W(PMe_3)_2$" was unstable with respect to W(IV) as **14**, a reduction of **12** led to the stable Mo(II) diphosphine, $(silox)_2Mo(PMe_3)_2$ (**17**). X-ray crystal structures of **10** (pseudo-O_h), **12** (square pyramidal), and **14** and **17** (distorted T_d) are reported. Calculations address the diamagnetism of **12** and **16**, and the distortion of **17** and its stability to cyclometalation in contrast to **14**.

Introduction

Recent investigations of group 5 niobium and tantalum species,[1,2] and group 6 molybdenum and tungsten compounds,[3,4] have focused on low-coordinate d^2 and d^3 complexes that reveal the influence of $nd_{z^2}/(n+1)s$ mixing[5,6] on structure and reactivity. Key syntheses of trigonal monoprismatic $(silox)_3MoCl$ and squashed tetrahedral $(silox)_3WCl$[3] led to the preparation of $(silox)_3MPMe_3$ (M = Mo, W; silox = ^{t}Bu$_3$SiO), $(silox)_3Mo$, and related C_{3v} derivatives including $(silox)_3MP$ (M = Mo, W).[4] The M(III) complexes are particularly interesting because steric and electronic features prevented generation of the typical metal−metal triply bonded compounds, whose chemistry comprises a significant fraction of the coordination chemistry of this oxidation state in group 6.[7,8]

Similar to molybdenum and tungsten(III), low-coordinate, mononuclear Mo(II) and W(II) compounds are difficult to prepare due to their propensity to form metal−metal bonds. Quadruple-bonded complexes readily form, and these occupy a historically important niche in inorganic coordination chemistry due to the presence of δ-bonding.[7,9] While the use of the silox (^{t}Bu$_3$SiO) ligand has enabled the synthesis

* Authors to whom correspondence should be addressed. E-mail: ptw2@cornell.edu (P.T.W.), tomc@unt.edu (T.R.C.).
† Cornell University.
‡ University of North Texas.

(1) Veige, A. S.; Slaughter, L. M.; Lobkovsky, E. B.; Wolczanski, P. T.; Matsunaga, N.; Decker, S. A.; Cundari, T. R. *Inorg. Chem.* **2003**, *42*, 6204–6224.
(2) Hirsekorn, K. F.; Hulley, E. B.; Wolczanski, P. T.; Cundari, T. R. *J. Am. Chem. Soc.* **2008**, *130*, 1183–1196.
(3) Kuiper, D. S.; Douthwaite, R. E.; Mayol, A.-R.; Wolczanski, P. T.; Lobkovsky, E. B.; Cundari, T. R.; Lam, O. P.; Meyer, K. *Inorg. Chem.* **2008**, *47*, 7139–7153.
(4) Kuiper, D. S.; Wolczanski, P. T.; Lobkovsky, E. B.; Cundari, T. R. *J. Am. Chem. Soc.* **2008**, *130*, 12931−12943.
(5) (a) Firman, T. K.; Landis, C. R. *J. Am. Chem. Soc.* **2001**, *123*, 11728–11742. (b) Landis, C. R.; Cleveland, T.; Firman, T. K. *J. Am. Chem. Soc.* **1998**, *120*, 2641–2649. (c) Landis, C. R.; Firman, T. K.; Root, D. M.; Cleveland, T. *J. Am. Chem. Soc.* **1998**, *120*, 1842–1854. (d) Weinhold, F.; Landis, C. R. *Valency and Bonding*; Cambridge University Press: Cambridge, U.K., 2005. (e) For a convenient plot of orbital energies vs *Z*, see Figure 15.39 in: Oxtoby, D. W.; Gillis, H. P.; Nachtrieb, N. H. *Principles of Modern Chemistry*, 5th ed.; Thomson Brooks/Cole: Florence, KY, 2002.
(6) Pyykkö, P. *Chem. Rev.* **1988**, *88*, 563–594.
(7) Cotton, F. A.; Walton, R. A. *Multiple Bonds Between Metal Atoms;* Oxford University Press: New York, 1993.
(8) (a) Chisholm, M. H. *Acc. Chem. Res.* **1990**, *23*, 419–425. (b) Chisholm, M. H.; Cotton, F. A. *Acc. Chem. Res.* **1978**, *11*, 356–362.
(9) Cotton, F. A.; Nocera, D. G. *Acc. Chem. Res.* **2000**, *33*, 483–490.

10.1021/ic8011958 CCC: $40.75
Published on Web 10/21/2008

Scheme 1

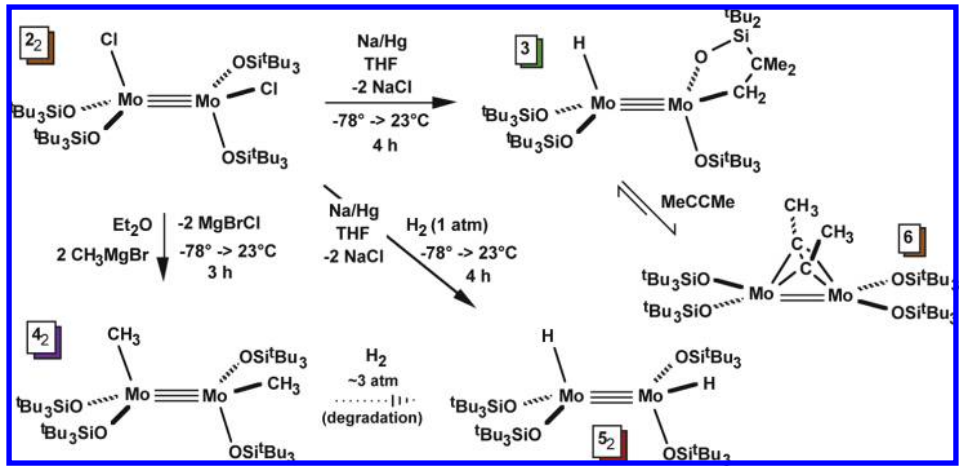

of numerous low-coordinate, low-valent compounds, "(silox)$_2$M" (M = Mo, W) is unlikely to be a stable entity, and even the quadruple-bonded "[(silox)$_2$M]$_2$" dimers are probably too reactive to isolate on the basis of previous W$_2$ chemistry. Efforts at generating [(silox)$_2$W]$_2$ resulted in cyclometalation to afford (silox)$_2$HWW(κ-O,C-OSi^{t}Bu$_2$CMe$_2$CH$_2$)(silox),[10] and the transient dimer is also the likely reactive species that degrades ethylene to [(silox)$_2$W]$_2$(μ-CH)$_2$ and dihydrogen via [(silox)$_2$W]$_2$(μ-CH)(μ-CH$_2$)(μ-H).[11] The first-row group 6 analogue, "(silox)$_2$Cr", exists as the siloxide-bridged dimer, [(^{t}Bu$_3$SiO)Cr]$_2$(μ-OSi^{t}Bu$_3$)$_2$;[12] hence, there is modest precedent for stabilizing group 6 M(II) centers in dimeric form.

During these studies, the use of PMe$_3$ has been extremely advantageous in trapping low-valent silox-containing intermediates prior to degradation or metal−metal bond formation.[1,4,13,14] Herein, efforts to generate low-coordinate, low-valent group 6 M(II) compounds are described, including efficient syntheses of critical starting materials, the successful generation of (silox)$_2$Mo(PMe$_3$)$_2$, and an analysis of its electronics via computation.

Results

Approaches to [(silox)$_2$Mo]$_2$. 1. Reduction and Methylation of [(silox)$_2$MoCl]$_2$. Although the putative D_{2d} [(silox)$_2$W]$_2$ transient dimer proved too reactive to isolate,[10] the lowered proclivity of Mo(II) to oxidize via CH oxidative addition was enough incentive to consider the synthesis of [(silox)$_2$Mo] (**1**$_2$). The synthesis of *gauche* C_2 [(^{t}Bu$_3$SiO)$_2$MoCl]$_2$ (**2**$_2$) from MoCl$_3$ and Na(silox) has been previously described,[3] and this was deemed an attractive starting material. As Scheme 1 illustrates, the reduction of **2**$_2$ unfortunately resulted in the cyclometalated derivative, (silox)$_2$HMoMo(κ-O,C-OSi^{t}Bu$_2$CMe$_2$CH$_2$)(silox) (**3**), which was isolated as a green-brown solid in 90% yield. ^{1}H NMR spectra of **3** revealed three silox groups, two singlets for the remaining *tert*-butyl groups, singlets for two Me groups, diastereotopic methylene hydrogens, and a hydride at δ 14.30, as Table 1 indicates.

Crystallization of crude **3** proved unsuccessful; hence, other methods of preparation were attempted. The addition of 2.0 equiv of MeMgBr in Et$_2$O to [(^{t}Bu$_3$SiO)$_2$MoCl]$_2$ (**2**$_2$), with subsequent filtration and recrystallization from pentane, afforded the purple dimethyl compound, [(^{t}Bu$_3$SiO)$_2$MoCH$_3$]$_2$ (**4**$_2$), in 85% yield. Its *gauche* C_2 symmetric structure[3,10] was substantiated by the presence of two inequivalent silox resonances in the ^{1}H NMR spectrum (δ 1.19, δ 1.28), equivalent methyl resonances (δ 3.48), and related ^{13}C{^{1}H} NMR spectral signals. The stoichiometric hydrogenation of **4**$_2$ to (silox)$_2$HMoMo(κ-O,C-OSi^{t}Bu$_2$CMe$_2$CH$_2$)(silox) (**3**) and 2 equiv of MeH could not be affected, and **4**$_2$ proved to be unreactive to 1 atm of H$_2$ at 23 °C. Upon extended thermolysis under excess H$_2$ at 70 °C, evidence of a dihydride was present, but continued heating or higher temperatures resulted in degradation.

2. Trapping of [(silox)$_2$Mo]$_2$. The reduction of [(^{t}Bu$_3$SiO)$_2$MoCl]$_2$ (**2**$_2$) with 2.0 equiv of Na/Hg in the presence of 1 atm of H$_2$ in THF resulted in the formation of reddish-brown [(^{t}Bu$_3$SiO)$_2$MoH]$_2$ (**5**$_2$). Two silox singlets in the ^{1}H NMR spectrum again revealed *gauche* C_2 symmetry of the dihydride,[10] and an additional resonance at δ 16.85 characterized the MoH units (Table 1). A strong ν(MoH) was observed at 1965 cm^{-1} in the infrared spectrum of **5**$_2$. In contrast to the tungsten analog,[10] **5**$_2$ could not be isolated by recrystallization from various hydrocarbon and ethereal solvents, and the presence of ~5% ^{t}Bu$_3$SiONa, ~3% ^{t}Bu$_3$SiOH, and residual THF were typically evident in its ^{1}H NMR spectrum. Unfortunately, the percentages of these impurities did not change when the reaction times were varied (3−48 h).

In an NMR tube experiment, (silox)$_2$HMoMo(κ-O,C-OSi^{t}Bu$_2$CMe$_2$CH$_2$)(silox) (**3**) was explored as an alternative means to generating the putative [(silox)$_2$Mo]$_2$ (**1**$_2$). With 1 equiv of 2-butyne as a trapping reagent, thermolysis at 100

(10) Miller, R. L.; Lawler, K. A.; Bennett, J. L.; Wolczanski, P. T. *Inorg. Chem.* **1996**, *35*, 3242–3253.
(11) Chamberlin, R. L. M.; Rosenfeld, D. C.; Wolczanski, P. T.; Lobkovsky, E. B. *Organometallics* **2002**, *21*, 2724–2735.
(12) Sydora, O. L.; Kuiper, D. S.; Wolczanski, P. T.; Lobkovsky, E. B.; Dinescu, A.; Cundari, T. R. *Inorg. Chem.* **2006**, *45*, 2008–2021.
(13) Rosenfeld, D. C.; Wolczanski, P. T.; Barakat, K. A.; Buda, C.; Cundari, T. R.; Schroeder, F. C.; Lobkovsky, E. B. *Inorg. Chem.* **2007**, *46*, 9715–9735.
(14) Veige, A. S.; Wolczanski, P. T.; Lobkovsky, E. B. *J. Chem. Soc., Chem. Comm.* **2001**, 2734–2735.

Table 1. ^{1}H, ^{13}C{^{1}H}, and ^{31}P NMR Spectral Assignments[a] for Diamagnetic Group 6 Siloxide Complexes

	^{1}H NMR (δ (J(Hz)), assmt)		^{13}C{^{1}H} NMR (δ,(J(Hz) assmt))		
compound	^{t}Bu	R/H etc.	Si*C*	SiC(CH_3)$_3$	R/H etc.
[(silox)$_2$MoCl]$_2$ (**2**$_2$)[b]	1.25		23.98	30.98	
	1.27		24.53	31.67	
(silox)$_2$HMoMo(silox)(κ-O,C−Si^{t}BuCMe$_2$CH$_2$) (**3**)	1.13	1.27, 1.37 (^{t}Bu)	24.42	30.74	23.94, 23.40 (Si*C*)
	1.24	1.54, 1.56 (Me)	24.06	31.23	23.85 (*C*Me$_2$)
	1.34	3.78 (d, 11, C*H*H)	23.21	31.24	29.89 (MoCH$_2$)
		3.86 (d, 11, CH*H*)			31.66, 31.93 (C(*C*H$_3$)$_3$)
		14.30 (MoH)			34.24, 34.43 (C(*C*H$_3$)$_2$)
[(silox)$_2$MoCH$_3$]$_2$ (**4**$_2$)	1.19	3.48 (Me)	24.18	31.38	48.27 (Me)
	1.28		24.66	31.41	
[(silox)$_2$MoH]$_2$ (**5**$_2$)[c]	1.22	16.85 (H)	23.20	30.79	
	1.31		23.97	31.40	
[(silox)$_2$Mo]$_2$(μ:η^2,η^2-C$_2$Me$_2$) (**6**)	1.05	3.17 (Me)			
	1.35				
(silox)$_2$Mo(NMe$_2$)$_2$ (**7**)	1.21	3.27 (NMe$_2$)	22.85	30.15	60.56 (N(CH$_3$)$_2$)
(silox)$_2$MoCl$_4$ (**8**)	1.28		26.11	30.69	
(silox)$_2$MoCl$_2$(PMe$_3$) (**12**)[d]	1.25	1.06 (d, 11,[e] PMe$_3$)	24.99	30.95	18.31 (32,[f] PMe$_3$)
(silox)$_2$HW(η^2-CH$_2$PMe$_2$)PMe$_3$ (**14**)[g]	1.31	1.25 (d, 10,[e] PMe)	24.00	31.46	19.63 (br, PMe)
	1.35	1.26 (d, 8,[e] PMe$_3$)	24.24	31.57	25.35 (21,[f] PMe)
		1.34 (d, 10,[e] PMe)			26.14 (32,[f] PMe$_3$)
		2.35 (ddd, 7, 7,[e] 5,[e] C*H*H)			
		4.83 (dd, 87,[e] 27,[e] 53,[h] WH)			
		5.05 (ddd, 14,[e] 7,[e] 7, CH*H*)			
(silox)$_2$WCl$_4$ (**15**)[b]	1.38		27.23	32.55	
(silox)$_2$WCl$_2$(PMe$_3$) (**16**)[i]	1.29	1.18 (d, 12,[e] PMe$_3$)	24.96	30.95	31.06 (36,[f] PMe$_3$)

[a] Benzene-d_6 unless otherwise noted; J_{HH} unless otherwise noted. [b] Taken from ref 3. [c] IR (nujol), n(MoH) = 1965 cm^{-1}. [d] ^{31}P NMR δ −6.35. [e] J_{PH}. [f] J_{PC}. [g] ^{31}P{^{1}H} NMR δ −3.01 (d with satellites, J_{PP} = 8, J_{WP} = 204), −33.16 (d with satellites, J_{PP} = 7, J_{WP} = 178). [h] From tungsten satellites, this is J_{WH}. [i] ^{31}P NMR δ −68.13 (J_{PW} = 610).

°C for 48 h produced only 80% [(silox)$_2$Mo]$_2$(μ:$\eta^2\eta^2$-C$_2$Me$_2$) (**6**), according to ^{1}H NMR analysis (K ∼ 460 M^{-1}; ΔG ° ∼ −4.5 kcal/mol). 2-Butyne-bridged **6** possesses a C_2 twist that is observed via two silox resonances in its ^{1}H NMR spectrum, just like its tungsten analogue.[11] Along with the formation of [(^{t}Bu$_3$SiO)$_2$MoH]$_2$ (**5**$_2$) from a reduction of [(^{t}Bu$_3$SiO)$_2$-MoCl]$_2$ (**2**$_2$), these results strongly suggest that [(silox)$_2$Mo]$_2$ (**1**$_2$) is a viable species, but unstable with respect to its cyclometalation product, **3**. Further trapping reactions with alkynes and olefins were not attempted with **3**, nor were any attempts made to isolate pure **6**. Unlike the alkyne scission that occurs in the thermolysis of [(silox)$_2$W]$_2$(μ:$\eta^2\eta^2$-C$_2$Me$_2$) at 80 °C,[11] **6** remained thermally stable to 120 °C.

Precursors to the (silox)$_2$Mo Core. 1. (silox)$_2$Mo-(NMe$_2$)$_2$. The aforementioned experiments suggested that [(silox)$_2$Mo]$_2$ (**1**$_2$) was not stable, and that cleavage of multiply bonded dimolybdenum complexes was unlikely to be a successful approach toward Mo(II) species. As a consequence, routes derived from mononuclear starting materials were sought. Despite its potential, the Mo(IV) tetraamide, Mo(NMe$_2$)$_4$, has not been routinely used as a starting material because its original synthesis—from MoCl$_5$ and LiMe$_2$—results in ∼10% yield and requires separation from [(Me$_2$N)$_3$Mo]$_2$.[15,16] The use of Mo(IV) starting materials MoCl$_4$(THF)$_2$ and MoCl$_4$(DME) gave modestly better yields (∼10−15%), and the use of Zr(NMe$_2$)$_4$ and Sn(NMe$_2$)$_4$ as nonreductive amide sources led to mostly diamagnetic product mixtures. The best procedure was determined to be the direct treatment of MoCl$_4$(OEt$_2$)$_2$ with a stoichiometric amount of LiNMe$_2$ in Et$_2$O, which afforded 25% purple Mo(NMe$_2$)$_4$ upon sublimation. The treatment of Mo(NMe$_2$)$_4$ with 2 equiv of (silox)H in pentane provided (silox)$_2$Mo-(NMe$_2$)$_2$ (**7**) as a maroon diamagnetic solid in 70% yield (eq 1).

$$\mathrm{Mo(NMe_2)_4} + 2\mathrm{HOSi^tBu_3} \xrightarrow[23\ ^\circ\mathrm{C},\ 30\ \mathrm{min}]{\text{pentane}} \underset{\mathbf{7}}{\mathrm{(silox)_2Mo(NMe_2)_2}} + \mathrm{HNMe_2} \quad (1)$$

Somewhat surprisingly, (silox)$_2$Mo(NMe$_2$)$_2$ (**7**) was remarkably unreactive toward NH$_3$, H$_2$PPh, 2,6-Ph$_2$-C$_6$H$_3$NH$_2$, and RNH$_2$ (R = adamantly, Si^{t}Bu$_3$) at 150 °C in C$_6$D$_6$. The diamide did react with MeI and TMSCl in C$_6$D$_6$, but only TMS-NMe$_2$ could be identified among many paramagnetic products in each reaction. As a consequence, molybdenum halides were revisited as potential starting materials.

2. *bis*-Silox Derivatives from MoCl$_5$. As in Weidenbruch's original report of silox-containing transition metal complexes,[17] the silanolysis of MoCl$_5$ was explored. Treatment of MoCl$_5$ with (silox)H in refluxing CCl$_4$ led to (silox)$_2$MoCl$_4$ (**8**) and (silox)$_2$MoCl$_3$ (**9**) in proportions that were highly dependent on the purity of the initial halide and the length of the reaction. During a 2 h procedure with an Ar purge, the ratio of **8**/**9** was roughly 1:4 on the basis of ^{1}H NMR integration of a singlet corresponding to a diamagnetic product at δ 1.28 in relation to a broad ($\nu_{1/2}$ ∼ 35 Hz) singlet at δ 1.36. Extended periods (>6 h) provided almost exclusively the Mo(VI) tetrachloride **8** in preference to the Mo(V) trichloride **9**, as shown in Scheme 2. Presumably, extended reaction times permitted a slower oxidation of **9** by CCl$_4$ to occur. Unfortunately, the greater reflux times

(15) Bradley, D. C.; Chisholm, M. H. *J. Chem. Soc. A* **1971**, 2741–2744.
(16) Chisholm, M. H.; Cotton, F. A.; Extine, M. W. *Inorg. Chem.* **1978**, *17*, 1329–1332.
(17) Weidenbruch, M; Pierrard, C.; Pesel, H. *Z. Naturforsch.* **1978**, *33B*, 1468–1471.

Scheme 2

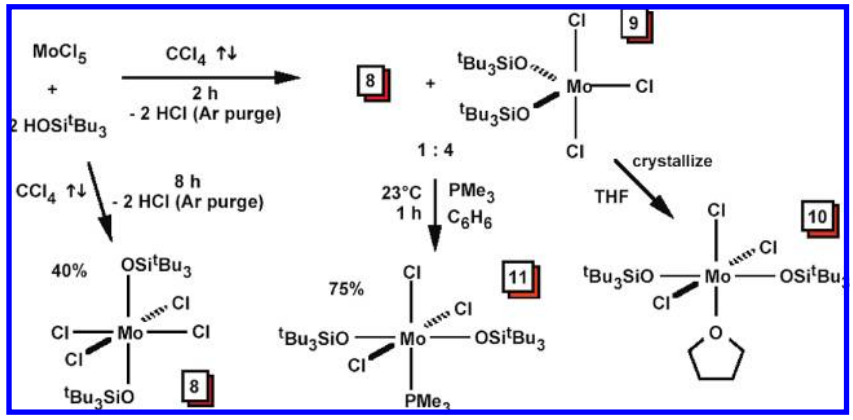

Table 2. Crystallographic Data for (silox)$_2$MoCl$_3$(THF) (**10**), (silox)$_2$MoCl$_2$(PMe$_3$) (**12**), (silox)$_2$HW(η^2-CH$_2$PMe$_2$)PMe$_3$ (**14**), and (silox)$_2$Mo(PMe$_3$)$_2$ (**17**)

	10[a]	**12**	**14**	**17**
formula	$C_{28}H_{62}O_3Si_2Cl_3Mo$	$C_{27}H_{63}O_2Si_2Cl_2PMo$	$C_{30}H_{72}O_2Si_2P_2W$	$C_{30}H_{72}O_2Si_2P_2Mo$
fw	705.27	673.79	766.88	678.94
space group	*C*2/*c*	$P2_1/n$	$P\bar{1}$	$P2_1/n$
Z	4	4	2	4
a, Å	8.7262(8)	8.5082(6)	8.6908(9)	9.2725(4)
b, Å	15.4639(17)	15.5481(10)	13.0276(16)	28.0138(13)
c, Å	27.145(2)	26.5089(17)	17.333(2)	15.0447(7)
α, deg	90	90	99.970(6)	90
β, deg	96.374(3)	97.070(3)	94.754(6)	90.252(3)
γ, deg	90	90	101.066(6)	90
V, Å^3	3640.3(6)	3480.1(4)	1883.2(4)	3907.9(3)
r_{calcd}, g cm^{-3}	1.287	1.286	1.352	1.152
μ, mm^{-1}	0.672	0.667	3.239	0.501
temp, K	173(2)	173(2)	173(2)	173(2)
λ (Å)	0.71073	0.71073	0.71073	0.71073
R indices [$I > 2\sigma(I)$][b,c]	$R_1 = 0.0340$	$R_1 = 0.0246$	$R_1 = 0.0438$	$R_1 = 0.0572$
	$wR_2 = 0.0841$	$wR_2 = 0.0647$	$wR_2 = 0.0957$	$wR_2 = 0.1191$
R indices (all data)[b,c]	$R_1 = 0.0516$	$R_1 = 0.0320$	$R_1 = 0.0660$	$R_1 = 0.0684$
	$wR_2 = 0.0876$	$wR_2 = 0.0662$	$wR_2 = 0.1017$	$wR_2 = 0.1251$
GOF[d]	1.102	1.124	1.006	1.008

[a] Half of a molecule of **10** constitutes an asymmetric unit. [b] $R_1 = \sum||F_o| - |F_c||/\sum|F_o|$. [c] $wR_2 = [\sum w(|F_o| - |F_c|)^2/\sum wF_o^2]^{1/2}$. [d] GOF (all data) = $[\sum w(|F_o| - |F_c|)^2/(n - p)]^{1/2}$, n = number of independent reflections, p = number of parameters.

also increased the amount of an impurity, which was spectroscopically identified as (silox)$_2$Mo(O)$_2$.[18] It is not certain whether the dioxo species is derived from impure starting material or whether the copious HCl produced as a byproduct helps dehydrate the glass reaction vessel, but it does limit the isolated yield of **8** to ~40%. The tungsten analogue, (silox)$_2$WCl$_4$, was produced in similar fashion from WCl$_6$, and (silox)$_2$WCl$_3$ can be generated from it via reduction.[3]

Attempts to separate (silox)$_3$MoCl$_3$ (**9**) from (silox)$_2$MoCl$_4$ (**8**) via fractional crystallization failed in most solvents, but in THF, orange-red crystals of a THF adduct, *mer*-(silox)$_2$MoCl$_3$(THF) (**10**), were produced in 40% yield. A more efficient means of producing a Mo(V) starting material involved treatment of the **8/9** mixture with PMe$_3$ to precipitate the nearly insoluble phosphine adduct, (silox)$_2$MoCl$_3$(PMe$_3$) (**11**), from benzene in ~75% yield on the basis of MoCl$_5$.

3. Structure of *mer*-(silox)$_2$MoCl$_3$(THF) (10). Table 2 provides the X-ray crystallographic data pertaining to *mer*-(silox)$_2$MoCl$_3$(THF) (**10**), while pertinent bond distances and angles are given in Table 3. Figure 1 shows that **10** is a nearly perfect octahedron with one chloride ligand and the THF opposite one another (180° by symmetry) and a set of *trans*-silox groups (179.42(8)°). The remaining *trans*-chlorides (172.86(2)°) are tipped slightly toward the THF (86.43(2)°), and the corresponding Cl1−Mo−Cl2 angles are 93.57(2)°. All remaining angles are within 1.2° of 90°, and the bond distances are normal for Mo(V), with a *d*(MoO) of 1.8348(12) Å and 2.3429(7) Å that describe the silox and THF interactions, respectively. The chloride opposite THF is slightly closer to Mo (2.3429(7) Å) than the others (2.369(2) Å), as expected from trans-influence arguments.

4. Synthesis of (silox)$_2$MoCl$_2$(PMe$_3$) (12). The phosphine adduct, (silox)$_2$MoCl$_3$(PMe$_3$) (**11**), proved to be a convenient starting material. The reduction of **11** with Na/Hg in diethyl ether with PMe$_3$ present (~3 equiv gave optimum yields) afforded the diamagnetic blue Mo(IV) complex, (silox)$_2$MoCl$_2$(PMe$_3$) (**12**), in 90% yield according to eq 2. In the ^{1}H NMR spectrum of **12**, the singlet corresponding to the silox was at δ 1.25, and a doublet attributed to the PMe$_3$ was observed at δ 1.06 (J_{PH} = 11 Hz). The ^{13}C{^{1}H} NMR

(18) Rosenfeld, D. C.; Kuiper, D. S.; Lobkovsky, E. B.; Wolczanski, P. T. *Polyhedron* **2006**, *25*, 251–258.

Table 3. Selected Bond Distances (Å) and Angles (deg) for *mer*-(silox)$_2$MoCl$_3$(THF) (**10**), (silox)$_2$MoCl$_2$(PMe$_3$) (**12**), (silox)$_2$HW(η^2-CH$_2$PMe$_2$)PMe$_3$ (**14**), and (silox)$_2$Mo(PMe$_3$)$_2$ (**17**)

	10[a]	**12**[b]	**14**[c]	**17**[d]
M−O1	1.8348(12)	1.8317(7)	1.918(3)	1.975(3)
M−O2		1.8358(7)	1.914(3)	1.943(3)
Mo−O(THF)	2.1676(17)			
Mo−Cl1	2.3689(5)	2.4277(3)		
Mo−Cl2	2.3429(7)	2.4424(3)		
M−P1		2.3933(3)	2.3537(13)	2.3374(13)
M−P2			2.3713(13)	2.3330(13)
W−C1			2.235(6)	
(P−C)$_{av}$		1.802(7)	1.801(38)	1.806(7)
(O−Si)$_{ave}$	1.7066(13)	1.691(3)	1.638(6)	1.616(5)
O1−M−O1′/2	179.42(8)	157.91(3)	104.87(13)	136.67(13)
O1−M−O(THF)	90.29(4)			
O1−Mo−Cl1	91.18(4)	90.43(3)		
O−Mo−Cl1′	88.85(4)			
O1−Mo−Cl2	89.71(4)	89.28(3)		
Cl1−Mo−O(THF)	86.43(2)			
Cl2−Mo−O(THF)	180			
O2−Mo−Cl1		90.48(3)		
O2−Mo−Cl2		88.71(3)		
Cl1−Mo−Cl1′	172.86(2)			
Cl1−Mo−Cl2	93.57(2)	177.11(2)		
P1−M−O1		100.57(3)	96.84(9)	96.85(10)
P1−M−O2		101.49(2)	132.79(9)	111.74(10)
P2−M−O1			134.62(9)	99.62(10)
P2−M−O2			96.83(10)	110.14(10)
P1−M−P2			96.74(5)	93.10(5)
P1−Mo−Cl1		89.81(2)		
P1−Mo−Cl2		93.08(2)		
O1−W−C1			132.33(19)	
O2−W−C1			91.04(19)	
P1−W−C1			45.47(17)	
P2−W−C1			85.56(18)	
W−P1−C1			63.7(2)	
W−P1−C2			136.4(3)	
W−P1−C3			118.23(18)	
W−C1−P1			70.8(2)	
M−O1−Si1	171.86(8)	163.57(5)	157.2(2)	152.2(2)
M−O2−Si2		158.85(5)	167.2(2)	175.1(2)

[a] The apical chloride is Cl2. [b] The Mo−P1−C's are 111.85(5)°, 112.08(5)°, and 117.93(5)°. [c] The W−P2−C angles are 114.1(2)°, 122.1(3)°, and 120.8(4)°; the C−P2−C angles are 90.1(4)°, 97.1(4)°, and 105.7(5)°; the C−P1−C angles are 109.7(4)°, 111.4(3)°, and 104.5(4)°. [d] The Mo−P1−C angles are 114.0(2)°, 114.9(2)°, and 123.8(2)°, and the Mo−P2−C angles are 114.8(2)°, 118.8(2)°, and 120.6(2)°.

spectrum was consistent with this formulation, and the ^{31}P NMR spectrum showed a single resonance at δ −6.35.

$$\underset{\mathbf{11}}{(\text{silox})_2\text{MoCl}_3(\text{PMe}_3)} \xrightarrow[\text{Et}_2\text{O, 23 °C, 4 h}]{\text{Na/Hg, 3PMe}_3\text{, − NaCl}} \underset{\mathbf{12}}{(\text{silox})_2\text{MoCl}_2(\text{PMe}_3)} \quad (2)$$

5. Structure of (silox)$_2$MoCl$_2$(PMe$_3$) (12). Structural details of (silox)$_2$MoCl$_2$(PMe$_3$) (**12**) can be found in Table 2, and core bond distances and angles are provided in Table 3. As Figure 2 illustrates, **12** is a square-pyramidal molecule with PMe$_3$ in the apical position, and *trans*-silox and *trans*-chlorides occupying the basal positions. There is a modest distortion—presumably steric—from a perfect square pyramid as the O−Mo−P angles average 101.0(7)°, while the Cl−Mo−P angles are 89.81(2)° and 93.08(2)°. All of the O−Mo−Cl angles within the base average 89.7(9)°, and the O−Mo−O and Cl−Mo−Cl angles are 157.91(3)° and 177.11(2)°, respectively. The *d*(MoCl) averages 2.435(10) Å, which is >0.06 Å longer than the *d*(MoCl) average in *mer*-(silox)$_2$MoCl$_3$(THF) (**10**). Taking the chlorides along the *x* axis, this lengthening may manifest 2e$^-$ occupation of the Cl → Mo dπ* bonding d$_{xz}$ orbital, rather than the π* component of the stronger π-donor siloxides (d$_{yz}$). The phosphine has a slight lean away from Cl2 (P1−Mo−Cl2 = 93.08(2)°, P1−Mo−Cl1 = 89.81(2)°), and the corresponding asymmetry in the C−P1−Mo angles (110.85(5)°, 112.08(5)°, and 117.93(5)°) is consistent with slight σ/π mixing to maximize Mo−P bonding.[4,13] The *d*(MoO) average is 1.834(3) Å, essentially the same as in **10**, and the *d*(MoP) is normal at 2.3933(3).

Approaches to the (silox)$_2$W Core. 1. Via (silox)$_3$WCl (13). The W(III) PMe$_3$ complex (silox)$_3$WPMe$_3$ was prepared via Na/Hg (∼1 equiv) reduction of (silox)$_3$WCl (**13**) in moderate yield (∼40%),[4] but **13** was discovered to be prone to overreduction. The product of a controlled reduction using 2 equiv of Na/Hg in the presence of 10 equiv of PMe$_3$ was the red hydride (silox)$_2$HW(η^2-CH$_2$PMe$_2$)PMe$_3$ (**14**; eq 3), which was isolated in only 15% yield via fractional crystallization despite being present in ∼90% yield according to ^{1}H NMR analysis. Its origin is likely to be the transient (silox)$_2$W(PMe$_3$)$_2$ (**15**) complex, which is expected to be susceptible to CH bond oxidative addition to its W(II) center.

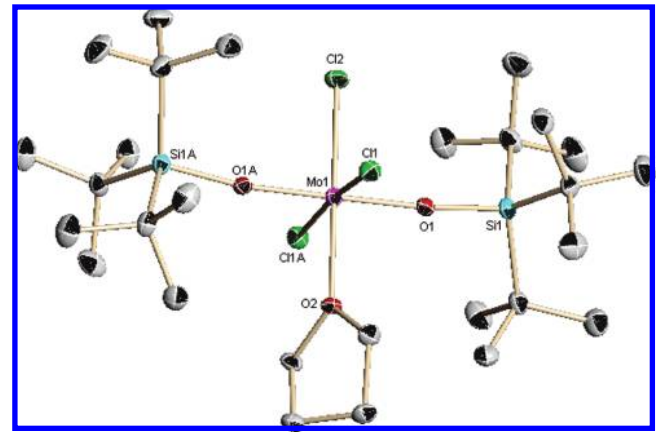

Figure 1. Molecular view of *mer*-(silox)$_2$MoCl$_3$(THF) (**10**).

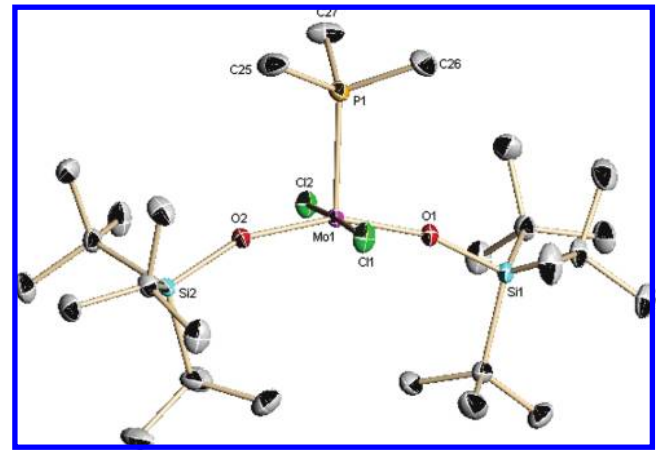

Figure 2. Molecular structure of (silox)$_2$MoCl$_2$(PMe$_3$) (**12**).

There is ample precedent for CH bond activation by W(II) in this manner.[19−22]

$$\underset{\mathbf{13}}{(\text{silox})_3\text{WCl}} \xrightarrow[\text{Et}_2\text{O, 24h, 23 °C}]{\text{2Na/Hg, 10PMe}_3\text{, − NaCl, − Na(silox)}} \underset{\mathbf{14}}{(\text{silox})_2\text{HW}(\eta^2\text{-CH}_2\text{PMe}_2)\text{PMe}_3} \quad (3)$$

The composition of the cyclometalated product, (silox)$_2$HW(η^2-CH$_2$PMe$_2$)PMe$_3$ (**14**), was initially determined by NMR spectroscopy, with the aid of correlation spectroscopy and heteronuclear multiple-quantum coherence experiments. Inequivalent silox groups were observed in the ^{1}H NMR spectrum in addition to diastereotopic methylene and PMe signals corresponding to the η^2-CH$_2$PMe$_2$ ligand. The hydride signal was located at δ 4.83 with 87 and 27 Hz coupling to the phosphorus atoms and J_{WH} = 57 Hz, as revealed by tungsten satellites (^{183}W, I = 1/2, 14.3%); a ν(WH) of 1820 cm^{-1} was observed in the IR spectrum of **14**.

2. (silox)$_2$WCl$_4$ (15) and (silox)$_2$WCl$_2$(PMe$_3$) (16). The separation difficulties of the process described above, and the low efficiency of removing a siloxide group, prompted an effort toward a better route to (silox)$_2$HW(η^2-CH$_2$PMe$_2$)PMe$_3$ (**14**). As previously discovered, silanolysis of WCl$_6$ can be used to produce (silox)$_2$WCl$_4$ (**15**) in 90% isolated yield, and it can be efficiently utilized as a starting material.

$$\underset{\mathbf{15}}{(\text{silox})_2\text{WCl}_4} \xrightarrow[\text{Et}_2\text{O, 23 °C, 4h}]{\text{2Na/Hg, 3PMe}_3\text{, − 2NaCl}} \underset{\mathbf{16}}{(\text{silox})_2\text{WCl}_2(\text{PMe}_3)} \quad (4)$$

$$\underset{\mathbf{15}}{(\text{silox})_2\text{WCl}_4} \xrightarrow[\text{Et}_2\text{O, 23 °C, 12h}]{\text{4Na/Hg, 3PMe}_3\text{, − 4NaCl}} \underset{\mathbf{14}}{(\text{silox})_2\text{HW}(\eta^2\text{-CH}_2\text{PMe}_2)\text{PMe}_3} \quad (5)$$

The reduction of **15** with 2 equiv of Na/Hg in the presence of 3 equiv of PMe$_3$ in diethyl ether generated the purple W(IV) (silox)$_2$WCl$_2$(PMe$_3$) (**16**) complex in 72% yield, as shown in eq 4. The structure of diamagnetic **16** is assumed to be analogous to its Mo congener (**12**) and its spectral parameters are listed in Table 1. One very unusual spectroscopic parameter was noted. The J_{WP}, as evidenced via satellite resonances (^{183}W, I = 1/2, 14.3%), is 610 Hz, a value considerably higher than that of (silox)$_3$WP ($^1J_{WP}$ = 162 Hz),[4] and only slightly less than the $^1J_{WP}$ of 649 Hz reported for the nearly linear (168.2(2)°) phosphinidene (*cis*-Cl$_2$)(CO){*trans*-(Ph$_2$MeP)$_2$}WP(2,4,6-^{t}Bu$_3$-C$_6$H$_2$) by Cowley et al.[23] This may be an indication of the significant 5d$_{z^2}$/6s mixing common to third row transition elements, since a hybrid orbital of this type would be utilized in bonding to the apical position of the presumed square pyramid. While (silox)$_2$WCl$_2$(PMe$_3$) (**16**) can be used as a precursor to (silox)$_2$HW(η^2-CH$_2$PMe$_2$)PMe$_3$ (**14**), it is even more efficient to reduce (silox)$_2$WCl$_4$ directly, as eq 5 indicates. With 4 equiv of Na/Hg in the presence of 3 equiv of PMe$_3$ in Et$_2$O, **14** was cleanly produced in 85% yield.

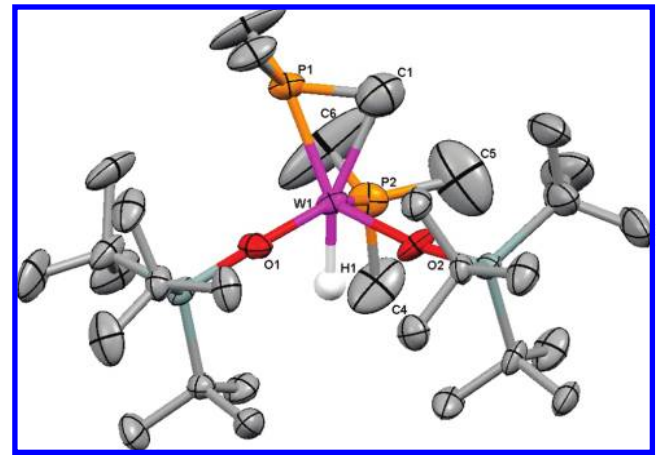

Figure 3. Molecular view of (silox)$_2$HW(η^2-CH$_2$PMe$_2$)PMe$_3$ (**14**) with hydride *placed* in most sterically probable location.

3. Structure of (silox)$_2$HW(η^2-CH$_2$PMe$_2$)PMe$_3$ (14). Data collection information pertaining to (silox)$_2$HW(η^2-CH$_2$PMe$_2$)PMe$_3$ (**14**) can be found in Table 2, and its distances and angles are listed in Table 3. As Figure 3 illustrates, **14** has a solid-state configuration consistent with the aforementioned NMR spectrum, including inequivalent siloxides that are adjacent (O1−W−O2 = 104.87(13)°) to one another, and a W(η^2-CH$_2$PMe$_2$) moiety that is roughly parallel to one WOSi unit (O2−W−P1 = 132.79(9)°, C1−W−O2 = 91.04(19)°), and perpendicular to the other (O1−W−P1 = 96.84(9)°, C1−W−O1 = 132.33(19)°) and the PMe$_3$ ligand (P1−W−P2 = 96.74(5)°, C1−W−P2 = 85.56(18)°). Ignoring the hydride, which could not be located, and counting the η^2-CH$_2$PMe$_2$ ligand as a single "site", the structure adopts a pseudo-T_d geometry with O1−W−P2 opened to 134.62(9)° to accommodate the PMe$_2$ fragment. With the η^2-CH$_2$PMe$_2$ ligand (W−P1−C1 = 63.7(2)°, P1−C1−W = 70.8(2)°, and C1−W−P1 = 45.47(17)°) taken as the apex, the hydride, when placed according to "best sterics" criteria, resides roughly equidistant from the PMe$_3$ (O2−W−P2 = 96.83(10)°) and the silox ligands (O1−W−O2 = 104.87(13)°). The distances in the structure appear normal, with a d(WP) of 2.3713(13) Å for the PMe$_3$ group, slightly longer than the 2.3537(13) Å of the η^2-CH$_2$PMe$_2$ ligand (d(WC) = 2.235(6) Å), and d(WO)'s of 1.914(3) and 1.918 (3) Å.

The (silox)$_2$Mo Core. 1. (silox)$_2$Mo(PMe$_3$)$_2$ (17) via Reduction. Although W(II) was not stabilized by a combination of silox and PMe$_3$, precedent suggested that a related

(19) (a) Green, M. L. H.; Parkin, G.; Mingquin, C.; Prout, K. *J. Chem. Soc., Chem. Commun.* **1984**, 1400–1402. (b) Green, M. L. H.; Parkin, G.; Chen, M.; Prout, K. *J. Chem. Soc., Dalton Trans.* **1986**, 2227–2236. (c) Green, M. L. H.; Parkin, G.; O'Hare, D.; Wong, L. L.; Derome, A. E. *J. Organomet. Chem.* **1986**, *317*, 61–68.

(20) (a) Buccella, D.; Tanski, J. M.; Parkin, G. *Organometallics* **2007**, *26*, 3275–3278. (b) Buccella, D.; Parkin, G. *J. Am. Chem. Soc.* **2006**, *128*, 16358–16364. (c) Churchill, D. G.; Janak, K. E.; Wittenberg, J. S.; Parkin, G. *J. Am. Chem. Soc.* **2003**, *125*, 1403–1420.

(21) (a) Gibson, V. C.; Grebenik, P. D.; Green, M. L. H. *J. Chem. Soc., Chem. Commun.* **1983**, 1101–1102. (b) Gibson, V. C.; Graimann, C. E.; Hare, P. M.; Green, M. L. H.; Bandy, J. A.; Grebenik, P. D.; Prout, K. *J. Chem. Soc., Dalton Trans.* **1985**, 2025–2035.

(22) Hirsekorn, K. F.; Veige, A. S.; Wolczanski, P. T. *J. Am. Chem. Soc.* **2006**, *128*, 2192–2193.

(23) Cowley, A. H.; Pellerin, B.; Atwood, J. L.; Bott, S. G. *J. Am. Chem. Soc.* **1990**, *112*, 6734–6735.

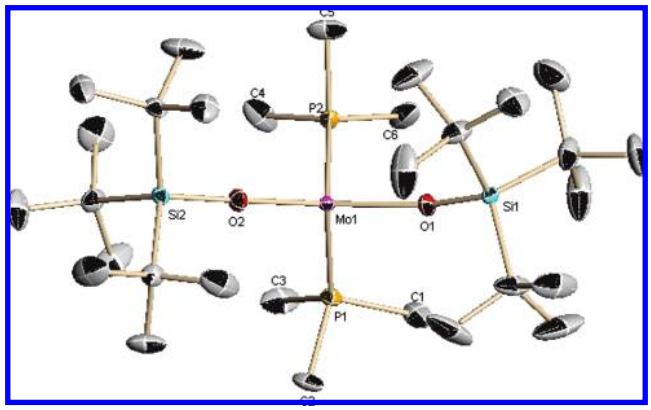

Figure 4. Molecular view of (^{t}Bu$_3$SiO)$_2$Mo(PMe$_3$)$_2$ (**17**).

attempt would be successful for Mo(II).[19−22,24] The reduction of (silox)$_2$MoCl$_2$(PMe$_3$) (**12**) with Na/Hg in Et$_2$O with 3 equiv of PMe$_3$ present afforded red (^{t}Bu$_3$SiO)$_2$Mo(PMe$_3$)$_2$ (**17**) in 68% yield upon crystallization from pentane. Compound **17** is paramagnetic, with a solution μ_{eff} of 2.6 at 23 °C, but NMR spectra were revealing. Two resonances were observed in the ^{1}H NMR spectrum at δ 2.33 ($\upsilon_{1/2}$ = 75 Hz) and δ 11.44 ($\upsilon_{1/2}$ = 120 Hz), while only one signal was apparent in the ^{13}C{^{1}H} NMR spectrum at δ 91.40 (C(*C*H$_3$)$_3$). The data appeared promising for an S = 1 Mo(II) species, but an X-ray crystal structure was necessary to confirm the composition.

$$\underset{\mathbf{15}}{(\text{silox})_2\text{MoCl}_2(\text{PMe}_3)} \xrightarrow[\text{Et}_2\text{O, 23 °C, 24h}]{\text{2Na/Hg, 3PMe}_3, -\text{2NaCl}} \underset{\mathbf{17}}{(^t\text{Bu}_3\text{SiO})_2\text{Mo(PMe}_3)_2} \quad (6)$$

2. Structure of (silox)$_2$Mo(PMe$_3$)$_2$ (17). Information on data collection regarding (^{t}Bu$_3$SiO)$_2$Mo(PMe$_3$)$_2$ (**17**) is available in Table 2, metric features are given in Table 3, and its pseudo-T$_d$ geometry is evident in Figure 4. Elongated *d*(MoO)'s of 1.943(3) and 1.975(3) Å provide testament to the low oxidation state of the complex, whereas the shorter *d*(MoP)'s of 2.3330(13) and 2.3374(13) Å give evidence of the backbonding that occurs when PMe$_3$ binds to Mo(II). On the basis of a pure tetrahedral geometry, a diamagnetic complex would not be surprising for a second row element,[25] but instead, **17** manifests certain distortions that do not appear to be steric in origin. The O−Mo−O angle is opened up to 136.67(13)°, whereas the P−Mo−P angle is closed down to 93.10(5)°, despite the cone angle of PMe$_3$ (118°)[26,27] being roughly the same as that of silox (∼120° (est)).[28] What is more curious is the asymmetry of the P−Mo−P plane to the O−Mo−O plane. The O1−Mo−P1 and O1−Mo−P2 angles are 96.85(10)° and 99.62(10)°, respectively, but the related O2−Mo−P1 and O2−Mo−P2 angles are significantly greater (111.74(10)° and 110.14(10)°, respectively). O1, P1, and P2 occupy fac positions of an octahedron, and O2 is leaning away from the phosphines in a manner that does not make sense on pure steric grounds.

Discussion

Synthetic Studies. It is not surprising that the stability of the dimolybdenum triple bond hampered the elaboration of Mo(III),[7,8] but the inability to manipulate (silox)$_2$Mo(NMe$_2$)$_2$ (**7**) was disappointing given the investment in improving the yield of Mo(NMe$_2$)$_4$.[15,16] Fortunately, a return to Weidenbruch's silanolysis routes[17] has enabled the ready preparation of silox halides of molybdenum and tungsten. Aside from some modest separation problems, the syntheses of (silox)$_2$MCl$_4$ (M = Mo, **8**; W, **15**),[3] (silox)$_2$MoCl$_3$ (**9**), and its derivatives have solved the problem of gaining an entryway into the chemistry of the second and third row transition metals of group 6.

(silox)$_2$Mo(PMe$_3$)$_2$ (17) versus (silox)$_2$HW(η^2-CH$_2$PMe$_2$)-PMe$_3$ (14). Similar to the case of (silox)$_3$M (M = Mo, W), where the molybdenum complex is isolable but the tungsten is not,[4] Mo(II) can be stabilized by the combination of silox and PMe$_3$,[1,4,13,14] whereas "(silox)$_2$W(PMe$_3$)$_2$" is prone to the oxidative addition of an internal CH bond.[19−22,24] These observations follow the periodic trend that third row transition elements are more easily oxidized than their second row congeners.[20] However, it is surprising that Mo(II) is stabilized in a four-coordinate environment. Now that Cotton and Schmid have debunked the claims of "Cl$_2$Mo(PMe$_3$)$_2$" (i.e., Cl$_2$Zn(PMe$_3$)$_2$),[29,30] (silox)$_2$Mo(PMe$_3$)$_2$ (**17**) is likely the only four-coordinate Mo(II) species known. Related use of 2,6-Ph$_2$-C$_6$H$_3$O by the groups of Parkin and Rothwell led to discovery of the η^6-Ph,η^1-O coordination mode, yielding the seven-coordinate [η^1-(η^6-2-Ph)(6-Ph)C$_6$H$_3$O]Mo(PR^{1}R$^2_2$)$_2$H (R^1 = R^2 = Me;[31] R^1 = Me, R^2 = Ph)[32] derivatives. These studies were preceded by the synthesis of octahedral *tert*-butoxide complexes by Chisholm et al. as (^{t}BuO)$_2$Mo(py)$_2$(CO)$_2$[33] and (^{t}BuO)$_2$Mo(bipy)$_2$.[34] Thiolates have also seen activity as ligands compatible with Mo(II) centers, but these ^{t}BuS$^-$,[35,36] 2,6-Ph$_6$-C$_6$H$_3$S$^-$, and 2,4,6-^{i}PrC$_6$H$_2$S$^-$[37] compounds all possess higher coordination numbers than four.

(24) (a) Murphy, V. J.; Parkin, G. *J. Am. Chem. Soc.* **1995**, *117*, 3522–3528. (b) Zhu, G.; Tanski, J. M.; Churchill, D. G.; Janak, K. E.; Parkin, G. *J. Am. Chem. Soc.* **2002**, *124*, 13658–13659.
(25) Figgis, B. N.; Hitchman, M. A. *Ligand Field Theory and Its Applications*; Wiley-VCH: New York, 2000.
(26) Tolman, C. A. *Chem. Rev.* **1977**, *77*, 313–348.
(27) Bunten, K. A.; Chen, L.; Fernandez, A. L.; Poë, A. J. *Coord. Chem. Rev.* **2002**, *233*, 41–51.
(28) Wolczanski, P. T. *Polyhedron* **1995**, *14*, 3335–3362.
(29) (a) Fromm, K.; Plaikner, M.; Hey-Hawkins, E. *Z. Naturforsch., B: Chem. Sci.* **1995**, *50*, 894–898. (b) Fromm, K.; Plaikner, M.; Hey-Hawkins, E. *Z. Naturforsch., B: Chem. Sci.* **1996**, *51*, 1669–1669.
(30) Cotton, F. A.; Schmid, G. *Polyhedron* **1996**, *15*, 4053–4059.
(31) Hascall, T.; Baik, M.-H.; Bridgewater Brian, M.; Shin Jun, H.; Churchill David, G.; Friesner Richard, A.; Parkin, G. *Chem Comm.* **2002**, 2644–2645.
(32) Kerschner, J. L.; Torres, E. M.; Fanwick, P. E.; Rothwell, I. P.; Huffman, J. C. *Organometallics* **1989**, *8*, 1424–1431.
(33) Chisholm, M. H.; Huffman, J. C.; Kelly, R. L. *J. Am. Chem. Soc.* **1979**, *101*, 7615–7617.
(34) Chisholm, M. H.; Huffman, J. C.; Rothwell, I. P.; Bradley, P. G.; Kress, N.; Woodruff, W. H. *J. Am. Chem. Soc.* **1981**, *103*, 4945–4947.
(35) Kamata, M.; Yoshida, T.; Otsuka, S.; Hirotsu, K.; Higuchi, T. *J. Am. Chem. Soc.* **1981**, *103*, 3572–3574.
(36) Kamata, M.; Yoshida, T.; Otsuka, S.; Hirotsu, K.; Higuchi, T.; Kido, M.; Tatsumi, K.; Hoffmann, R. *Organometallics* **1982**, *1*, 227–230.
(37) Bishop, P. T.; Blower, P. J.; Dilworth, J. R.; Zubieta, J. A. *Polyhedron* **1986**, *5*, 363–367.

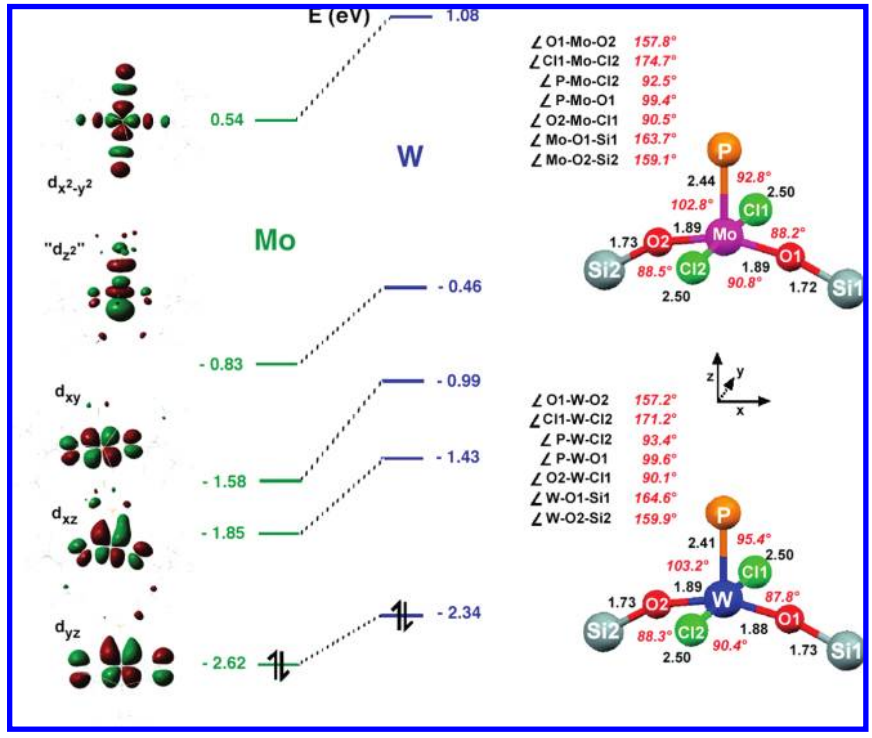

Figure 5. Calculated geometries and d-orbital splitting diagrams of (silox)$_2$MoCl$_2$PMe$_3$ (**12′**) and (silox)$_2$WCl$_2$PMe$_3$ (**16′**). Distances (black) are in angstroms; angles are in *italicized red.*

As for the cyclometalation of PMe$_3$ to afford (silox)$_2$HW(η^2-CH$_2$PMe$_2$)PMe$_3$ (**14**), this CH bond activation was first observed for tungsten by Green et al. in their attempt to prepare "W(PMe$_3$)$_6$".[19,21] The cyclometalation product (Me$_3$P)$_4$HW(η^2-CH$_2$PMe$_2$) was isolated instead. Later efforts by Parkin demonstrated that the Mo^0 center of (Me$_3$P)$_6$Mo is less prone to activating the CH bond of a PMe$_3$ ligand than its tungsten counterpart.[24]

Electronic Structures. 1. (silox)$_2$MCl$_2$PMe$_3$ (M = Mo, 12; W, 16). The X-ray crystal structure determination of (silox)$_2$MoCl$_2$PMe$_3$ (**12**) confirmed its expected square-pyramidal arrangement, but the diamagnetism observed for **12** and its third row congener (silox)$_2$WCl$_2$PMe$_3$ (**16**) was not an obvious consequence. Figure 5 illustrates the d-orbital splitting diagrams for the full models (**12′** and **16′**) as determined from high-level quantum mechanics/molecular mechanics calculations (QM/MM).[38−43] The calculated structure (**12′**) essentially reproduces the geometry determined by the crystal structure, except that the bond lengths are ∼0.04−0.06 Å longer. The tungsten analogue (**16′**) has a virually identical arrangement, with the exception of a significantly shorter *d*(WP) of 2.41 Å (*d*(MoP) = 2.44 Å), which is in concert with its anomalously large J_{WP} of 610 Hz.

The ordering of the orbitals portrayed in Figure 5 is standard, and the spread of energies is greater for W (3.42 eV) relative to the second row element (3.16 eV), as predicted on the basis of the slightly larger radial extent of the 5d orbitals. The slightly better σ and π overlaps for the third row metal are reflected in the generally greater gaps between each orbital pair. The lowest orbital, d_{yz}, is π^* with respect to the MCl bonds and π^b to phosphorus. There is a considerable gap (Mo, 0.77 eV; W, 0.91 eV) between d_{yz} and the next orbital, d_{xz}, that explains the diamagnetism. This is in part due to a modest amount of metal−oxygen σ^* character to the orbital, which is primarily metal−oxygen π^* and MP π-bonding. The cant of the siloxides relative to PMe$_3$ (e.g., P−Mo−O ∼ P−W−O ∼ 101°) turns on the σ antibonding character and elevates the orbital considerably, since it approaches the d_{xy} π^* orbital in energy (Mo, 0.30 eV; W, 0.44 eV). It is interesting to note that d_{xy} has virtually no MCl π^* character but possesses a considerable metal−oxygen π^* interaction. The d_{z^2} orbital for W is slightly

(38) Frisch, M. J.; Trucks, G. W.; Schlegel, H. B.; Scuseria, G. E.; Robb, M. A.; Cheeseman, J. R.; Montgomery, J. A., Jr.; Vreven, T.; Kudin, K. N.; Burant, J. C.; Millam, J. M.; Iyengar, S. S.; Tomasi, J.; Barone, V.; Mennucci, B.; Cossi, M.; Scalmani, G.; Rega, N.; Petersson, G. A.; Nakatsuji, H.; Hada, M.; Ehara, M.; Toyota, K.; Fukuda, R.; Hasegawa, J.; Ishida, M.; Nakajima, T.; Honda, Y.; Kitao, O.; Nakai, H.; Klene, M.; Li, X.; Knox, J. E.; Hratchian, H. P.; Cross, J. B.; Bakken, V.; Adamo, C.; Jaramillo, J.; Gomperts, R.; Stratmann, R. E.; Yazyev, O.; Austin, A. J.; Cammi, R.; Pomelli, C.; Ochterski, J. W.; Ayala, P. Y.; Morokuma, K.; Voth, G. A.; Salvador, P.; Dannenberg, J. J.; Zakrzewski, V. G.; Dapprich, S.; Daniels, A. D.; Strain, M. C.; Farkas, O.; Malick, D. K.; Rabuck, A. D.; Raghavachari, K.; Foresman, J. B.; Ortiz, J. V.; Cui, Q.; Baboul, A. G.; Clifford, S.; Cioslowski, J.; Stefanov, B. B.; Liu, G.; Liashenko, A.; Piskorz, P.; Komaromi, I.; Martin, R. L.; Fox, D. J.; Keith, T.; Al-Laham, M. A.; Peng, C. Y.; Nanayakkara, A.; Challacombe, M.; Gill, P. M. W.; Johnson, B.; Chen, W.; Wong, M. W.; Gonzalez, C.; Pople, J. A. *Gaussian 03*, revision C.02; Gaussian, Inc.: Wallingford CT, 2004.
(39) Parr, R. G.; Yang, W. *Density-functional Theory of Atoms and Molecules*; Oxford University Press: Oxford, U.K., 1989.
(40) Stevens, W. J.; Krauss, M.; Basch, H.; Jasien, P. G. *Can. J. Chem.* **1992**, *70*, 612–630.
(41) Hirsekorn, K. F.; Veige, A. S.; Marshak, M. P.; Koldobskaya, Y.; Wolczanski, P. T.; Cundari, T. R.; Lobkovsky, E. B. *J. Am. Chem. Soc.* **2005**, *127*, 4809–4830.
(42) Vreven, T.; Morokuma, K. *J. Comput. Chem.* **2000**, *21*, 1419–1432.
(43) Rappé, A. K.; Casewit, C. J.; Colwell, K. S.; Goddard, K. S., III; Skiff, W. M. *J. Am. Chem. Soc.* **1992**, *114*, 10024–10035.

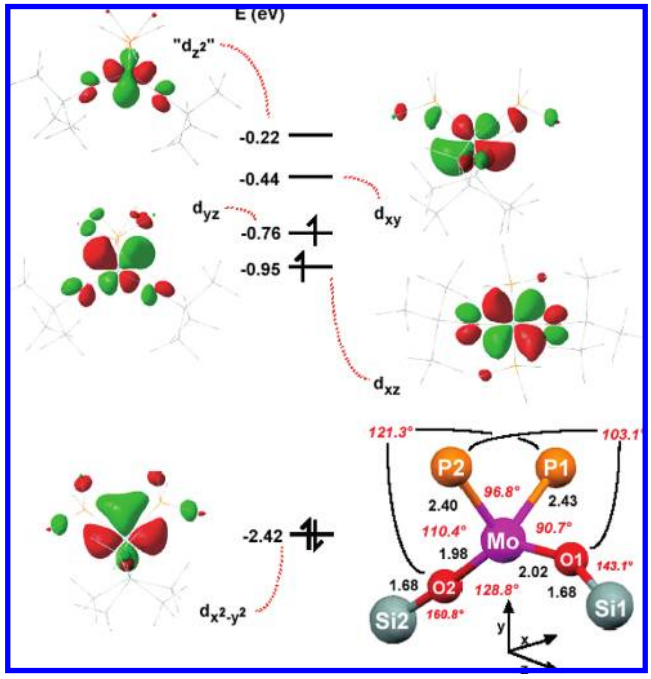

Figure 6. Calculated geometry and d-orbital splitting diagram of $(silox)_2Mo(PMe_3)_2$ (**17′**). Distances (black) are in angstroms; angles are in *italicized red.*

higher—relative to d_{yz}—than in Mo, perhaps indicative of the greater 6s involvement in WP bonding.[3] Note that the $d_{x^2-y^2}$ orbital has more MCl than metal−oxygen σ^* character, as expected on the basis of ΔE_{MX} arguments.

2. $(silox)_2Mo(PMe_3)_2$ (17). In a pseudo-T_d geometry, a "3 over 2" orbital arrangement would be expected to generate a low-spin ($S = 0$) d^4 configuration for a second or third row transition element.[25] In an attempt to better understand the observed $S = 1$ electronic state of $(silox)_2Mo(PMe_3)_2$ (**17**), high-level QM/MM calculations were conducted on the full model (**17′**).[38−43] While most of the major geometric features of the structure were effectively modeled by **17′**, the tilt of the P−Mo−P plane with respect to the O−Mo−O plane was not. Instead of tilting toward one silox ligand, the P−Mo−P plane has a much greater twist with respect to the O−Mo−O plane (O−Mo-*P* = 90.7° and 103.1° vs 110.4° and 121.3°), as Figure 6 reveals, and the calculated *d*(MoO) and *d*(MoP) are 0.03−0.04 Å and 0.07−0.10 Å greater, respectively. The geometric distortions occurred whether or not the crystal structure coordinates or a geometry generated from a molecular-mechanics-based conformational search was used to initiate the QM/MM-based geometry optimization. There is no obvious rationale for the angular discrepancies, and such subtleties are unlikely to alter the electronics to a great extent. The calculated P−Mo−P angle of 96.8° and O−Mo−O of 128.8° are also off by ∼3.7° and ∼ 7.8°, respectively, but the general features of the core are similar to the X-ray crystal structure and may simply indicate that **17** lies in a shallow minimum, whereby its angular changes are sensitive to the chemical environment.

The calculations reproduce the $S = 1$ ground state implicated by the solution magnetism of $(silox)_2Mo(PMe_3)_2$ (**17**), and corresponding singlet and quintet excited states are 2.3 and 13.8 kcal/mol above the triplet, respectively. A perusal of the orbitals in Figure 6 reveals nothing obvious that would cause the "twist" described above, so the contention that subtle bonding interactions are at play appears reasonable. The lowest orbital in the ligand field is best construed as $d_{x^2-y^2}$, and it is at −2.42 eV relative to the two singly occupied d_{xz} (−0.95 eV) and d_{yz} (−0.76 eV) orbitals. It is clear that $d_{x^2-y^2}$ has a significant Mo(dπ) → P(d/σ^*) backbonding component, while d_{xz} and d_{yz} carry the brunt of the O(pπ) → Mo(dπ)* antibonding interaction of the silox ligands, and d_{yz} has some σ^* character. At −0.44 eV and −0.22 eV are d_{xy} and "d_{z^2}", and these are σ^* towards the phosphines and the silox oxygens, respectively, although the low symmetry renders the latter orbital rather difficult to identify. The orbital energies must be treated with caution, as density functional theory (DFT) is prone to error in comparing filled versus half-filled versus empty orbitals,[44] but the expected "3 over 2" configuration is not apparent. By opening the O−Mo−O angle, d_{yz} becomes significantly less σ^* in character and is lower in energy, but the penalty is greater π^* character in d_{xz}, which is higher in energy; the proximity of the two leads to the $S = 1$ ground state, and their ∼0.19 eV separation is not enough to overcome a pairing energy. Thus "3 over 2" becomes "2 over 2 over 1", with $d_{x^2-y^2}$ greatly stabilized by the backbonding interaction, and through mixing with "d_{z^2}", which takes any σ^* character away.

Conclusions

The combination of $^tBu_3SiO$ (silox) and PMe_3 again proves to make a potent duo in the synthesis of low-coordinate, low-oxidation-state species via the stabilization of Mo(II) as $(silox)_2Mo(PMe_3)_2$ (**17**). This combination is unable to overcome the propensity of W(II) to oxidation; hence, the related "$(silox)_2W(PMe_3)_2$" formula is found as the PMe_3 cyclometalation product, $(silox)_2HW(\eta^2\text{-}CH_2PMe_2)PMe_3$ (**14**).

Experimental Section

General Considerations. All manipulations were performed using either glovebox or high vacuum line techniques. Hydrocarbon solvents containing 1−2 mL of added tetraglyme and ethereal solvents were distilled under nitrogen from purple sodium benzophenone ketyl and vacuum-transferred from the same prior to use. Benzene-d_6 was dried over activated 4 Å molecular sieves, vacuum-transferred, and stored under N_2. All glassware was oven-dried, and NMR tubes for sealed tube experiments were additionally flame-dried under a dynamic vacuum. $MoCl_5$ was obtained from Strem Chemical, and $MoCl_4(THF)_2$, $MoCl_3(THF)_3$,[45] and $MoCl_4(OEt_2)_2$,[46] were prepared according to literature procedures, as were $[(^tBu_3SiO)_2MoCl]_2$ (**2**$_2$), $(silox)_3WCl$ (**2**-Cl), and $(silox)_2WCl_4$ (**15**).[3]

NMR spectra were obtained using Varian XL-400, INOVA-400, and Unity-500 spectrometers, and chemical shifts are reported relative to benzene-d_6 (^1H, δ 7.15; $^{13}C\{^1H\}$, δ 128.39). Infrared spectra were recorded on a Nicolet Impact 410 spectrophotometer

(44) Zhang, G.; Musgrave, C. B. *J. Phys. Chem. A* **2007**, *111*, 1554–1561.
(45) Dilworth, J. R.; Zubieta, J. *Inorg. Synth.* **1986**, *24*, 193–194.
(46) Stoffelbach, F.; Saurenz, D.; Poli, R. *Eur. J. Inorg. Chem.* **2001**, *269*, 9–2703.

interfaced to a Gateway PC, or a Nicolet Avatar 370 DTGS spectrophotometer interfaced with an IBM ThinkPad. Solution magnetic measurements were conducted via Evans' method in C_6D_6 unless otherwise noted.[47] Elemental analyses were performed by Oneida Research Services, Whitesboro, New York, or Robertson Microlit Laboratories, Madison, New Jersey.

Procedures. 1. (silox)$_2$HMoMo(κ-O,C-OSi^{t}Bu$_2$CMe$_2$CH$_2$)-(silox) (3). To a 100 mL flask containing 1.00 g (1.78 mmol) of [(^{t}Bu$_3$SiO)$_2$MoCl]$_2$ (**2$_2$**) and 4.52 g of Na/Hg (0.95%, 1.87 mmol) was distilled 50 mL of THF at −78 °C. The solution was allowed to warm slowly from −78 to 23 °C. After the green-brown solution was stirred for 4 h at 23 °C, all volatiles were removed *in vacuo*. The reaction mixture was triturated three times with 10 mL of hexanes and filtered in hexanes. The removal of all volatiles yielded 0.843 g (0.80 mmol, 90%) of **3** as a green-brown solid. IR (nujol mull, Na/Cl, cm^{-1}): 1945 (υ, MoH). Anal. calcd for $C_{50}H_{108}Cl_2Mo_2O_4Si_4$: C, 54.61; H, 10.50. Found: C, 54.24; H, 10.65.

2. [(^{t}Bu$_3$SiO)$_2$MoCH$_3$]$_2$ (4$_2$). To a 100 mL flask containing 1.00 g (0.889 mmol) of **2$_2$** was distilled 20 mL of Et_2O at −78 °C. CH_3MgBr (0.6 mL, 3.0 M in Et_2O) was added via syringe. The solution was allowed to warm to 23 °C and was stirred for 3 h. The flask was evacuated and the reaction mixture stripped of all volatiles. The resulting dusty-purple solid was dissolved in 50 mL of pentane and filtered, and the salt cake was repeatedly washed until no traces of product remained. The filtrates were concentrated to ∼5 mL, cooled to −78 °C, and filtered to give 0.818 g (0.755 mmol, 85%) of **4** as dusty-purple microcrystals. Anal. calcd for $C_{50}H_{108}Cl_2Mo_2O_4Si_4$: C, 55.42; H, 10.60. Found: C, 54.89; H, 10.76.

3. [(^{t}Bu$_3$SiO)$_2$MoH]$_2$ (5$_2$). To a 100 mL round-bottom flask containing 2.00 g (1.78 mmol) of **2$_2$** and 9.04 g of Na/Hg (0.95%, 3.73 mmol) was distilled 50 mL of THF at −78 °C. The solution was exposed to 1 atm of H_2 and allowed to warm slowly from −78 to 23 °C. After the red-brown solution was stirred for 4 h at 23 °C, all volatiles were removed in vacuo, and the reaction mixture was filtered in hexanes. The removal of all volatiles yielded 1.78 g (1.69 mmol, 95%) of **5$_2$** as a red-brown solid. IR (nujol mull, Na/Cl, cm^{-1}): 1965 (ν(MoH)). Anal. calcd for $C_{50}H_{108}Cl_2Mo_2O_4Si_4$: C, 54.61; H, 10.50. Found: C, 54.24; H, 10.65.

4. [(silox)$_2$Mo]$_2$(μ:$\eta^2$$\eta^2$-C$_2Me_2$) (6). A NMR tube attached to a needle valve adaptor was charged with a solution of **3** (30 mg, 0.028 mmol) in 0.65 mL of C_6D_6. The tube was fitted with a 180° needle valve and freeze−pump−thaw degassed three times. 2-Butyne (176 Torr, 0.28 mmol) was transferred via a calibrated 30.1 mL gas bulb. The tube was sealed and heated for 48 h at 100 °C. Partial conversion (80%) was seen by ^{1}H NMR spectroscopy, but 20% of the starting material remained even after continued thermolysis (8 h, 120 °C).

5. Mo(NMe$_2$)$_4$. To a 1 L three-neck round-bottom flask containing 30 g (0.59 mol) of $LiNMe_2$ was vacuum-transferred 300 mL of Et_2O. The $LiNMe_2$ solution was cooled to 0 °C, and a suspension of $MoCl_4(OEt_2)_2$[46] (55 g, 0.142 mol) in 150 mL of Et_2O was cannulated into the ice-cold $LiNMe_2$ solution. The reaction mixture was stirred at 0 °C for 4 h and then stirred at 23 °C for 48 h. The Et_2O was removed from the brown reaction mixture *in vacuo*, and the flask was fitted with a condenser. The surface of the condenser was cooled with a dry ice/acetone mixture, and the residue was heated to 80 °C for 2 h at 10^{-3} Torr. The resulting purple solid (7.80 g) deposited on the condenser was collected, and the process was repeated to give an additional 1.88 g for a combined yield of 25%. ^{1}H NMR (C_6D_6, 400 MHz): δ 3.27.

6. (silox)$_2$Mo(NMe$_2$)$_2$ (7). To a 100 mL flask containing 2.00 g (7.34 mmol) of Mo(NMe$_2$)$_4$ and 3.17 g (14.7 mmol) of ^{t}Bu$_3$SiOH was distilled 30 mL of pentane at −78 °C. The solution developed a deep maroon color upon warming. After stirring for 30 min, the solution was filtered and stripped of all volatiles. The solid was redissolved in minimal pentane (∼5 mL), cooled to −78 °C, and filtered to give 2.73 g (5.13 mmol, 70%) of **7** as maroon microcrystals. ^{1}H NMR (C_6D_6, 400 MHz): δ 1.21 (s, ^{t}Bu, 27H), 3.27 (s, N(CH$_3$)$_2$, 6H). ^{13}C{^{1}H} NMR (C_6D_6, 400 MHz): δ 23.84 (*C*(CH$_3$)), 23.99 (*C*(CH$_3$)), 30.88 (C(*C*H$_3$)), 31.42 (C(*C*H$_3$)). Anal. calcd for $C_{29}H_{66}N_2MoO_2Si_2$: C, 65.59; H, 12.53; N, 5.28. Found: C, 65.43; H, 12.63; N, 5.11.

7. (silox)$_2$MoCl$_4$ (8) and (silox)$_3$MoCl$_3$ (9) in 1:4 Ratio. To a 500 mL flask containing 10.0 g of ^{t}Bu$_3$SiOH (46.2 mmol) and 6.94 g of $MoCl_5$ (25.4 mmol) was vacuum-transferred 250 mL of CCl_4 at −78 °C. The dark purple suspension evolved copious amounts of HCl gas as the reaction mixture warmed to 23 °C and changed to a deep red color. The removal of HCl was further affected by the periodic exposure of the reaction mixure to a liquid-nitrogen-cooled trap under static vacuum for 1 h (∼15 cycles of HCl removal). The reaction mixture was then heated in a 45 °C water bath under a static vacuum with occasional evacuation of the vacuum manifold (∼15 min intervals). The reaction mixture was then stripped of all volatiles and assayed by ^{1}H NMR to reveal a 1:4 mixture of (^{t}Bu$_3$SiO)$_2$MoCl$_4$ (**8**) and (^{t}Bu$_3$SiO)$_2$MoCl$_3$ (**9**), respectively.

8. (silox)$_2$MoCl$_4$ (8). To a 250 mL flask containing 5.00 g of ^{t}Bu$_3$SiOH (23.1 mmol) and 6.31 g of $MoCl_5$ (23.1 mmol) was vacuum-transferred 100 mL of CCl_4 at −78 °C. The purple suspension was warmed to 23 °C under a heavy argon purge and allowed to stir for an hour. The deep red solution containing a dark precipitate was then heated to 65 °C under a gentle argon purge for 8 h. The red reaction mixture was stripped of all volatiles, and the soluble portion was redissolved in 150 mL of CCl_4. The reaction mixture was filtered, and the filtrates were concentrated to ∼15 mL. The red solution was cooled to 0 °C for 30 min and filtered to give 3.09 g of **8** (40%). Anal. calcd for $C_{24}H_{54}Cl_4MoO_2Si_2$: C, 43.11; H, 8.14. Found: C, 42.77; H, 8.39.

9. *mer*-(silox)$_2$MoCl$_3$(THF) (10). Procedure 6 was followed to obtain **8/9** in a ∼1:4 ratio. A small portion of the mixture (0.250 g) was taken up in 25 mL of THF, and the resulting solution was filtered, leaving behind a dark red solid (presumably **8**). The red solution was allowed to evaporate at room temperature until crystals were seen to form. Small orange-red crystals of **10** were isolated by decanting the remaining mother liquor (0.088 g, 40%). The reaction was not optimized. ^{1}H NMR (C_6D_6, 300 MHz): δ 0.95 (27 H, $\nu_{1/2} \approx 117$ Hz), 1.92 (4 H, $\nu_{1/2} \approx 102$ Hz). ^{13}C{^{1}H} NMR (C_6D_6, 500 MHz): δ 37.35 (C(*C*H$_3$)$_3$ $\nu_{1/2} \approx 625$ Hz). Anal. calcd for $C_{28}H_{62}Cl_3MoO_3Si_2$: C, 47.68; H, 8.86. Found: C, 47.31; H, 8.43.

10. (silox)$_2$MoCl$_3$(PMe$_3$) (11). Procedure 6 was followed to obtain **8/9** in a ∼1:4 ratio. The product mixture was redissolved in 300 mL of CCl_4 and filtered, leaving behind a small amount of dark solid. The CCl_4 was removed *in vacuo*, and the reaction mixture was suspended in 100 mL of Et_2O. The transfer of 2 equiv of PMe_3 (stoichiometry based on ^{t}Bu$_3$SiOH consumed) via calibrated gas bulb into the red suspension at −78 °C resulted in a bright orange solid and a green solution upon warming to 23 °C. The reaction mixture was stirred for 1 h and filtered, and the filter cake was washed to give bright orange (^{t}Bu$_3$SiO)$_2$MoCl$_3$(PMe$_3$)

(47) (a) Evans, D. F. *J. Chem. Soc.* **1959**, 2003–2005. (b) Schubert, E. M. *J. Chem. Educ.* **1992**, *69*, 62.

(**11**; 12.29 g, 75%). The formulation is tentative and based on EA and reactivity studies. Anal. calcd for $C_{36}H_{82}MoO_3Si_3$: C, 45.72; H, 8.95. Found: C, 44.70; H, 8.02.

11. (silox)$_2$MoCl$_2$(PMe$_3$) (12). To a 100 mL round-bottom flask containing 2.43 g of **11** (3.43 mmol) and 9.12 g of Na/Hg amalgam (1.1 equiv, 3.77 mmol) was vacuum-transferred ~40 mL of Et_2O at −78 °C. PMe_3 (3 equiv, 10.29 mmol) was transferred to the reaction mixture via calibrated gas bulb. The reaction mixture was warmed to 23 °C and stirred vigorously for 4 h. The orange suspension slowly turned green and then blue during the course of reaction. The blue suspension was stripped of all volatiles, and the Hg^0 was decanted. To the reaction mixture was transferred 50 mL of toluene. The blue solution was filtered, and the filter cake was washed with toluene until no trace of color remained. The blue filtrates were stripped of all volatiles; 20 mL of Et_2O was transferred into the flask, and the suspension was filtered to give microcrystalline **12** (2.08 g, 90%). Anal. calcd for $C_{27}H_{63}MoO_2PSi_2$: C, 48.13; H, 9.42. Found: C, 47.81; H, 9.13.

12. (silox)$_2$WCl$_2$(PMe$_3$) (16). To a 100 mL flask containing 1.00 g of (silox)$_2$WCl$_4$ (**15**; 1.32 mmol) and 6.72 g of Na/Hg amalgam (2.1 equiv, 2.78 mmol Na) was vacuum-transferred ~40 mL of Et_2O at −78 °C. PMe_3 (3 equiv, 3.96 mmol) was transferred to the reaction mixture via calibrated gas bulb. The reaction mixture was warmed to 23 °C and stirred vigorously for 4 h. The red suspension slowly turned purple throughout the course of the reaction. The purple suspension in purple solution was stripped of all volatiles, and the Hg^0 was decanted. To the reaction mixture was transferred 50 mL of toluene. The purple solution was filtered, and the filter cake was washed with toluene until no trace of color remained. The purple filtrates were stripped of all volatiles; 20 mL of Et_2O was transferred into the flask, and the suspension was filtered to give microcrystalline **26** (0.724 g, 72%). Anal. calcd for $C_{27}H_{63}O_2PSi_2W$: C, 42.58; H, 8.34. Found: C, 42.19; H, 8.02.

13. (silox)$_2$HW(η^2-CH$_2$PMe$_2$)PMe$_3$ (14). a. From (silox)$_2$WCl$_2$(PMe$_3$) (16). To a 100 mL round-bottom flask containing 1.00 g of **16** (1.16 mmol) and 5.73 g of Na/Hg (2.37 mmol) was vacuum-transferred 50 mL of Et_2O at −78 °C. PMe_3 (10 equiv, 11.6 mmol) was vacuum-transferred into the reaction mixture via calibrated gas bulb. The reaction mixture was allowed to warm to 23 °C and stir for 24 h. The red solution with white precipitate was stripped of all volatiles; the mercury was decanted, and the reaction mixture was dissolved and filtered in 50 mL of pentane. The removal of solvent in vacuo resulted in a mixture of red solid **14** and $NaOSi^tBu_3$. Pure red **14** (0.133 g, 0.173 mmol) was isolated by fractional crystallization from a slowly evaporating Et_2O solution at −30 °C.

b. From (silox)$_2$WCl$_4$(15). To a 100 mL round-bottom flask containing 2.00 g of **15** (2.64 mmol) and 26.2 g of Na/Hg (10.8 mmol) was vacuum-transferred 50 mL of Et_2O at −78 °C. PMe_3 (3 equiv of 7.92 mmol) was vacuum-transferred into the −78 °C reaction mixture via calibrated gas bulb. The dark red suspension was allowed to warm to 23 °C and stirred for 12 h. Within the first hour of the reduction, a dramatic color change to a green-brown solution with orange precipitate and then to a purple solution with a purple precipitate occurred. The reaction mixture gradually turned to red over the remaining reaction time. The reaction mixture was stripped of all volatiles; the Hg^0 was decanted, and the red solid was dissolved in 50 mL of pentane. The reaction mixture was filtered and the pentane removed in vacuo. The red solid was dissolved in minimal Et_2O and recrystallized at −30 °C over 12 h to give 1.72 g of **14** (2.24 mmol, 85%). Anal. calcd for $C_{30}H_{72}O_2P_2Si_2W$: C, 46.99; H, 9.46. Found: C, 46.55; H, 9.66.

14. (^{t}Bu$_3$SiO)$_2$Mo(PMe$_3$)$_2$ (17). To a 100 mL round-bottom flask containing 1.83 g of **12** (2.72 mmol) and 13.83 g of Na/Hg amalgam (2.1 equiv, 5.71 mmol Na) was vacuum-transferred ~50 mL of Et_2O at −78 °C. PMe_3 (3 equiv, 8.16 mmol) was transferred to the reaction mixture via calibrated gas bulb. The reaction mixture was warmed to 23 °C and stirred for 24 h. The blue reaction mixture slowly turned red throughout the course of the reaction. All volatiles were removed in vacuo, and the Hg^0 was decanted. Pentane (30 mL) was transferred to the reaction mixture, and the deep red solution was filtered. The red filtrates were concentrated to ~2 mL, and the red product was crystallized by slow evaporation of the saturated solution at −30 °C for 18 h. The small amount of solution remaining was removed, yielding 1.26 g (68%) of **17**. ^{1}H NMR (C_6D_6, 300 MHz): δ 2.33 ($\nu_{1/2}$ = 75 Hz), 11.44 ($\nu_{1/2}$ = 120 Hz). $^{13}C\{^1H\}$ NMR (C_6D_6, 500 MHz): δ 91.40 ($C(CH_3)_3$). Anal. calcd for $C_{27}H_{63}O_2PSi_2W$: C, 42.58; H, 8.34 Found: C, 42.19; H, 8.02. μ_{eff} (293 K) = 2.6 μ_B(C_6D_6).

15. Single-Crystal X-Ray Diffraction Studies. Upon isolation, the crystals were covered in polyisobutylene and placed under a 173 °C N_2 stream on the goniometer head of a Siemens P4 SMART CCD area detector system (graphite-monochromated Mo Kα radiation, λ = 0.71073 Å). The structures were solved by direct methods (SHELXS). All non-hydrogen atoms were refined anisotropically unless stated, and hydrogen atoms were treated as idealized contributions (Riding model).

16. *mer*-(silox)$_2$MoCl$_3$(THF) (10). A yellow block (0.6 × 0.35 × 0.15) was obtained from tetrahydrofuran. A total of 14 811 reflections were collected with 4409 being symmetry-independent (R_{int} = 0.0406), and 3302 were greater than 2$\sigma(I)$. The data were corrected for absorption by SADABS, and the refinement utilized $w^{-1} = \sigma^2(F_o^2) + (0.0399p)^2 + 0.2684p$, where $p = (F_o^2 + 2F_c^2)/3)$.

17. (silox)$_2$MoCl$_2$(PMe$_3$) (12). A blue rod (0.5 × 0.4 × 0.3) was obtained from diethyl ether. A total of 29 927 reflections were collected, with 8586 being symmetry-independent (R_{int} = 0.0252), and 7143 were greater than 2$\sigma(I)$. The data were corrected for absorption by SADABS, and the refinement utilized $w^{-1} = \sigma^2(F_o^2) + (0.0316p)^2 + 0.6198p$, where $p = (F_o^2 + 2F_c^2)/3)$.

18. (silox)$_2$HW(η^2-CH$_2$PMe$_2$)PMe$_3$ (14). A red rod (0.2 × 0.05 × 0.03) was obtained from diethyl ether. A total of 32 273 reflections were collected, with 6351 being symmetry-independent (R_{int} = 0.0914), and 4775 were greater than 2$\sigma(I)$. The data were corrected for absorption by SADABS, and the refinement utilized $w^{-1} = \sigma^2(F_o^2) + (0.0470p)^2 + 0.0000p$, where $p = (F_o^2 + 2F_c^2)/3)$. The PMe_3 group was partially disordered by rotation along the W−P bond. The hydride H atom was not visible on a difference Fourier map. It was placed using a "sterically most feasible" model.

19. (^{t}Bu$_3$SiO)$_2$Mo(PMe$_3$)$_2$ (17). A red plate (0.2 × 0.15 × 0.03) was obtained from pentane. A total of 25 756 reflections were collected, with 4052 being symmetry-independent (R_{int} = 0.0728), and 3529 were greater than 2$\sigma(I)$. The data were corrected for absorption by SADABS, and the refinement utilized $w^{-1} = \sigma^2(F_o^2) + (0.0403p)^2 + 16.2911p$, where $p = (F_o^2 + 2F_c^2)/3)$.

Computational Methods. Calculations were performed on full silox-decorated models using the Gaussian 03 package.[38] DFT, specifically the BLYP functional, was utilized for all simulations.[39] The transition metals and heavy main group atoms (Si and P) were described with the Stevens effective core potentials and attendant valence basis sets (VBSs).[40] This scheme, dubbed CEP-31G, entails a valence triple-ζ description for the transition metals, and a

double-ζ VBS for the main group elements. The 6-31G(d) all-electron basis set was used for C, H, and O atoms. All main group VBSs are augmented with a d polarization function (C(ξ_d) = O(ξ_d) = 0.8; Si(ξ_d) = 0.3247; P(ξ_d) = 0.37). This level of theory was selected on the basis of a series of test calculations on the singlet and triplet states of $Nb(OH)_3$, $Ta(OH)_3$,[1] and their olefin adducts.[41]

Full silox models were studied using hybrid QM/MM techniques within the ONIOM framework.[42] The QM region of M(silox)$_3$(X) complexes contained the transition metal, the O and Si atoms of the silox group, and the entire X group (if present). The QM level of theory employed is that described above. The remainder of the molecule, that is, the *tert*-butyl groups of silox, was modeled with the universal force field.[43]

Full geometry optimizations without any metric or symmetry restrictions were employed to obtain the minima in this research. All of the resultant stationary points were characterized as true minima (i.e., no imaginary frequencies) by calculation of the energy Hessian. Enthalpic and entropic corrections to the total electronic energy were calculated using harmonic vibrational frequencies determined at the same level of theory employed for geometry optimization and are calculated at 1 atm and 298.15 K.

Closed- and open-shell species were described with the restricted and unrestricted Kohn−Sham formalisms, respectively, with no evidence of spin contamination for the latter.

Acknowledgment. We thank the National Science Foundation (CHE-0415506, (PTW)), the US Dept. of Energy (DE-FG02-03ER15490 (TRC)), and Cornell University for financial support.

Supporting Information Available: CIF files of **10**, **12**, **14**, and **17**. This material is available free of charge via the Internet at http://pubs.acs.org.

IC8011958